ARMY RESEARCH LABORATORY

A Hybrid Supersonic/Subsonic Trajectory Model for Direct Fire Applications

by Paul Weinacht

ARL-TR-5574 **June 2011**

NOTICES

Disclaimers

The findings in this report are not to be construed as an official Department of the Army position unless so designated by other authorized documents.

Citation of manufacturer's or trade names does not constitute an official endorsement or approval of the use thereof.

Destroy this report when it is no longer needed. Do not return it to the originator.

Army Research Laboratory
Aberdeen Proving Ground, MD 21005-5066

ARL-TR-5574 **June 2011**

A Hybrid Supersonic/Subsonic Trajectory Model for Direct Fire Applications

Paul Weinacht
Weapons and Materials Research Directorate, ARL

REPORT DOCUMENTATION PAGE	Form Approved OMB No. 0704-0188

1. REPORT DATE *(DD-MM-YYYY)*	2. REPORT TYPE	3. DATES COVERED (From - To)
June 2011	Final	2009–2010

4. TITLE AND SUBTITLE
A Hybrid Supersonic/Subsonic Trajectory Model for Direct Fire Applications

5a. CONTRACT NUMBER

5b. GRANT NUMBER

5c. PROGRAM ELEMENT NUMBER

6. AUTHOR(S)
Paul Weinacht

5d. PROJECT NUMBER
IL1612618AH

5e. TASK NUMBER

5f. WORK UNIT NUMBER

7. PERFORMING ORGANIZATION NAME(S) AND ADDRESS(ES)
U.S. Army Research Laboratory
ATTN: RDRL-WML-E
Aberdeen Proving Ground, MD 21005-5066

8. PERFORMING ORGANIZATION REPORT NUMBER
ARL-TR-5574

9. SPONSORING/MONITORING AGENCY NAME(S) AND ADDRESS(ES)

10. SPONSOR/MONITOR'S ACRONYM(S)

11. SPONSOR/MONITOR'S REPORT NUMBER(S)

12. DISTRIBUTION/AVAILABILITY STATEMENT
Approved for public release; distribution is unlimited.

13. SUPPLEMENTARY NOTES

14. ABSTRACT
A simple but accurate method of determining the trajectory of projectiles that traverse a flight regime that includes supersonic and subsonic flight is presented. Closed-form analytical solutions for the important trajectory parameters such as the time-of-flight, velocity, gravity drop and wind drift are developed based on a power-law description of the drag variation with Mach number. The method demonstrates that the free-flight trajectory can be characterized in terms of five parameters; the muzzle velocity, muzzle retardation, a power-law exponent that describes the drag variation in supersonic flight, the transition Mach number where the flight transitions from supersonic to subsonic flight and the retardation at the transition velocity. The accuracy and simplicity of the method makes it very useful for preliminary design or performance assessment studies where rapid prediction of projectile trajectories is desired. Sample results are presented for the M855 projectile fired from the M16A2 rifle and a 9-mm pistol bullet fired from a handgun to demonstrate the viability of the method.

15. SUBJECT TERMS
projectiles, trajectory, aeroballistics, flight mechanics

16. SECURITY CLASSIFICATION OF:			17. LIMITATION OF ABSTRACT	18. NUMBER OF PAGES	19a. NAME OF RESPONSIBLE PERSON
a. REPORT	b. ABSTRACT	c. THIS PAGE			Paul Weinacht
Unclassified	Unclassified	Unclassified	UU	40	19b. TELEPHONE NUMBER (*Include area code*) 410-306-0800

Standard Form 298 (Rev. 8/98)
Prescribed by ANSI Std. Z39.18

Contents

List of Figures

List of Tables

Acknowledgments

The author wishes to acknowledge the U.S. Army PM-Maneuver Ammunition Systems for funding and supporting significant portions of this particular effort.

1. Introduction

Several recent studies have demonstrated there is a need for characterizing the free-flight performance of direct-fire systems including combat rifles, pistols, and sniper weapons. For many of these systems, combat rifles for example, the trajectory is characterized by supersonic flight over the useful operational range of the weapon system. Recent studies (*1*, *2*) have provided a framework for examining the free-flight trajectory within the constraints of supersonic flight. The basis of this approach is a simple but accurate method for predicting the trajectories for high-velocity direct-fire munitions (*1*). The method allows the trajectories to be characterized in terms of three parameters: the muzzle velocity, the muzzle retardation (or velocity fall-off) and a parameter defining the shape of the drag curve. The method provides an excellent means of assessing exterior ballistic performance in a conceptual design environment where details of the designs have not been completely defined or in assessment studies where the simple and rapid predictions of the trajectory are desired. Although developed for supersonic flight, the method also allows the prediction of trajectories in subsonic flight where the drag coefficient is constant with Mach number.

While the existing method has proved very useful, there are some applications where the trajectory involves supersonic flight during early phases of the trajectory and subsonic flight later in the trajectory as the projectile slows due to drag. Example applications include pistol and long range rifle systems. This report documents the extension of the power-law approach to trajectories with both supersonic and subsonic flight.

In the following sections, the analytical approach for solving the three degree-of-freedom (3DOF) trajectory equations is briefly described and benchmarked with numerical predictions of the trajectory of the 5.56-mm M855 projectile typically fired from the M16 and M4 rifles and 9-mm ball projectile fired from a pistol. The M855 projectile example demonstrates the performance of the method in an application where the projectile flight is primarily supersonic but reaches subsonic velocity later in flight. The 9-mm ball projectile example illustrates a case where the transition from supersonic to subsonic flight occurs in the middle of a typical flight. Both examples demonstrate the performance and accuracy of the method.

2. Technical Approach

The flat-fire trajectory of a projectile can be characterized as follows (*3*):

$$\begin{bmatrix}\text{The Complete}\\ \text{Flat Fire Trajectory}\end{bmatrix}=\begin{bmatrix}\text{The Flat Fire}\\ \text{Point Mass Trajectory}\end{bmatrix}+\begin{bmatrix}\text{Lateral}\\ \text{Throwoff}\end{bmatrix}+\begin{bmatrix}\text{Aerodynamic}\\ \text{Jump}\end{bmatrix}+\begin{bmatrix}\text{Epicyclic}\\ \text{Swerve}\end{bmatrix}+\begin{bmatrix}\text{Drift}\\ \end{bmatrix} \quad (1)$$

Of the trajectory components in equation 1, the flat-fire point-mass trajectory accounts for the most dominant characteristics of the trajectory and is most heavily influenced by the mass and drag characteristics of the projectile. It includes such effects as gravity drop and crosswind drift. It is this portion of the trajectory that is the focus of the current modeling approach. The aerodynamic jump and lateral throwoff of the projectile produce angular deviations of the flight path from the intended line of flight due to launch disturbances and mass asymmetries within the projectile, respectively. Bias errors associated with these effects are normally removed through the rifle zeroing process. These effects can also produce random errors that contribute to the ammunition dispersion. Normally, these effects would not be considered in any detail in a conceptual design process as the relative magnitude of these effects can only be quantified later in the design cycle. Additionally, the relative magnitude of the lateral throwoff is heavily influenced by manufacturing quality considerations. The epicyclic swerve represents fluctuating motions of the projectile about the trajectory due to the angular motion of the projectile. For a stable projectile, these motions are typically small relative to the mean path of the projectile. The drift produces a small horizontal deflection of the projectile that is fairly consistent from shot to shot. The deflection is typically small compared with crosswind drift.

The flat-fire point-mass trajectory can be obtained by solving the point-mass or 3DOF equations, which are obtained from Newton's second law. The flat-fire point-mass equations assume that the transverse aerodynamic forces such as the lift and Magnus forces are small and that the Coriolis acceleration due to the earth's rotation can be neglected. Neglecting the transverse aerodynamic forces is typically a good assumption if the total yaw of the projectile is small. Using this approach, the projectile is characterized by its muzzle velocity, mass, and the variation of its drag coefficient with Mach number. The lateral displacement of the projectile due to crosswind effects can be predicted using the classical crosswind drift formula, which is obtained from an analytical integration of the 3DOF equations (*4*). This is a general formula that does not make any specific assumptions regarding the functional form for the drag coefficient variation with Mach number. The up- and down-range wind effects are generally assumed to be small in comparison to the crosswind drift. With the lateral displacement due to crosswind drift obtained from the classical crosswind drift formula, the 3DOF equations can be reduced to a set of 2DOF differential equations shown in equations 2–9.

$$m\frac{dV_x}{dt} = -\frac{1}{2}\rho V^2 S_{ref} C_D \frac{V_x}{V}, \tag{2}$$

$$m\frac{dV_y}{dt} = -\frac{1}{2}\rho V^2 S_{ref} C_D \frac{V_y}{V} - mg, \tag{3}$$

$$\frac{ds_x}{dt} = V_x, \tag{4}$$

$$\frac{ds_y}{dt} = V_y, \tag{5}$$

The initial conditions are:

$$V_x(t=0) = V_0 \cos\theta_0, \tag{6}$$

$$V_y(t=0) = V_0 \sin\theta_0, \tag{7}$$

$$s_x(t=0) = 0, \tag{8}$$

$$s_y(t=0) = 0, \tag{9}$$

Typically, the integration of these equations is performed numerically since the equations are nonlinear and the functional form for the drag coefficient may be arbitrary. However, it is possible to obtain analytical solutions of these equations under the assumption of direct fire using an assumed form of the drag coefficient variation with Mach number (*1*).

2.1 Power Law Drag Model

For supersonic flight, it can be shown that the drag coefficient variation with Mach number can be modeled as a function of Mach number to a power as shown in equation 10. For constant atmospheric conditions, the sound speed is constant, and the Mach number and velocity are directly proportional. In this case, the drag coefficient varies with Mach number and velocity in the same manner.

$$C_D \propto \frac{1}{M^n} \propto \frac{1}{V^n}. \tag{10}$$

Figure 1 shows the variation of the drag coefficient with Mach number for the 5.56-mm M855. The firing tables branch (FTB), ARDEC "aeropack" data (*5*) used to construct firing tables for the round are shown along with aerodynamic spark range data (*6*). The fit of the FTB aeropack drag coefficient data in the supersonic regime obtained using the power-law formulation in equation 10 is also shown. The computed exponent for the M855 is 0.53 for the range between Mach 2.8 (muzzle velocity) and Mach 1.1. The power-law fit shows excellent agreement over this Mach number range.

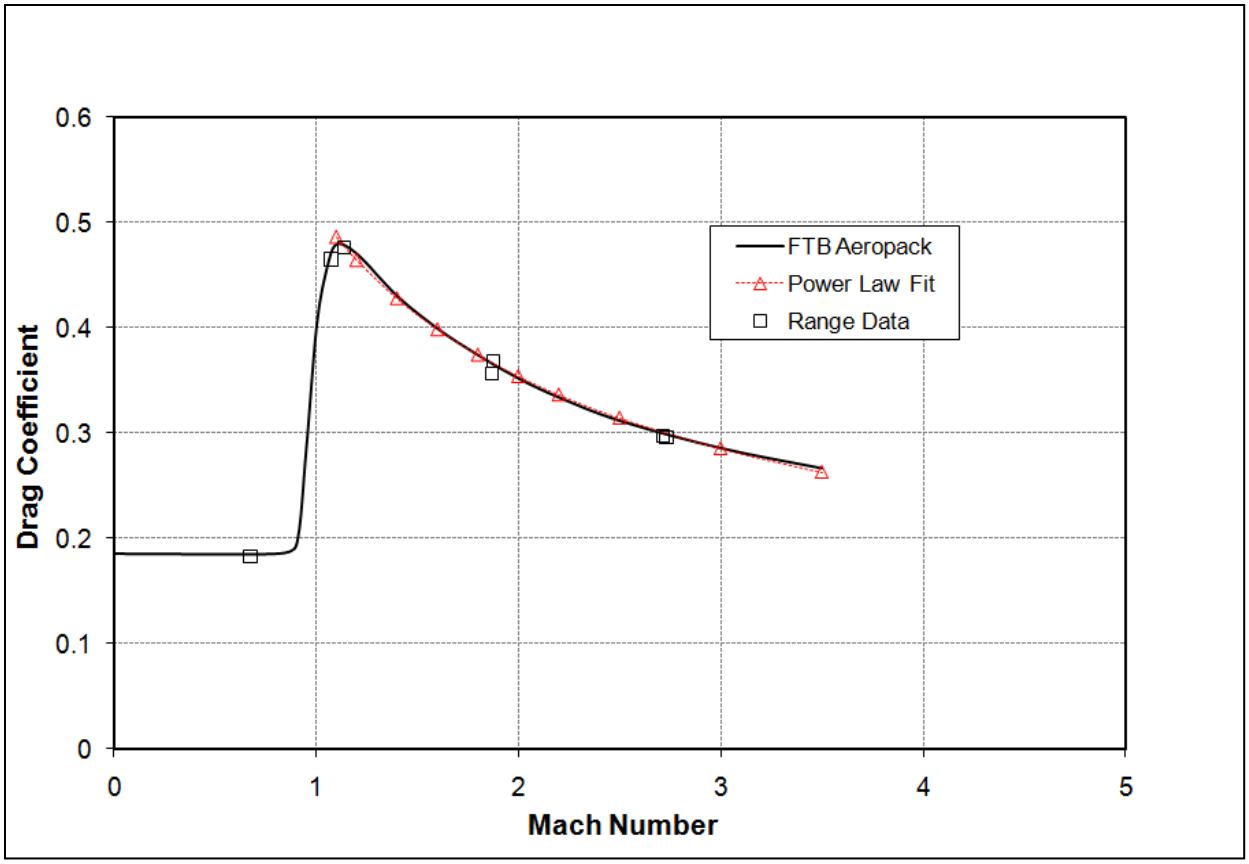

Figure 1. Supersonic power-law drag coefficient model compared with aeropack and range data for the M855.

Reference 1 examined the drag coefficient variation of a wide variety of munitions and found that the drag coefficient exponent varied between 0.0 and 1.0 for supersonic flight. This was further confirmed in reference 2 specifically for small arms ammunition and a correlation developed for small arms ammunition relating the drag coefficient exponent to the aeroballistic form factor. In general, as small arms projectiles become more blunt and less streamlined, the drag coefficient exponent decreased.

For subsonic flight (nominally $M < 0.8$), the projectile exhibits a constant drag coefficient with Mach number as shown in figure 1. This type of variation of the drag coefficient can also be modeled with the functional relationship shown in equation 10 where n = 0. Thus, a projectile flying in either purely supersonic flight or subsonic flight can be modeled using a power-law approach. However, there are classes of bullets that may have supersonic launch velocities but slow to subsonic velocities due to the action of drag. For trajectories like these, the approach of reference 1 cannot be applied directly; however, it appears that this approach can be adapted to address trajectories with mixed supersonic and subsonic flights.

It should be noted that extrapolating the power-law approach into the subsonic regime using the typical supersonic (n > 0) power-law drag variation results in a drag coefficient that approaches infinity as the velocity goes to zero. This produces a rapid deterioration in the accuracy of the

approach once the projectile reaches the subsonic regime. Thus, determination of the trajectory with mixed supersonic and subsonic flight requires the appropriate modeling of the drag variation in each regime.

For trajectories that consist of both supersonic and subsonic flight, the projectile must also traverse the transonic regime (nominally between Mach 0.8 and 1.1 with the largest drag variation seen between Mach 0.9 and 1.0). For the purposes of modeling many aspects of the trajectory of a bullet, the details of the drag behavior within the transonic regime can often be ignored. Instead, the trajectory can be modeled with a hybrid supersonic/subsonic drag model where the transition between supersonic and subsonic flight occurs somewhere within the transonic regime. It is noted that more complex models, such as numerical 3DOF models, can incorporate the details of the transonic regime as part of the modeling approach. However, there is very often a lack of drag data to completely support detailed modeling in this regime. Instead, a supersonic and subsonic drag data are often combined with a hypothetical transonic drag behavior that allows a continuous drag variation across supersonic, transonic, and subsonic flight. Thus, the accuracy of these numerical methods in the transonic regime is strongly dependent on the quality of the drag data used as input to these models and the results obtained with a hybrid supersonic/subsonic drag model may provide comparable accuracy when the details of the transonic drag behavior is somewhat uncertain.

Figure 2 shows an example of the hybrid supersonic/subsonic power-law drag model for the M855 projectile compared with FTB, ARDEC "aeropack" data (*5*). The computed power-law exponent for the M855 is 0.53 for the supersonic regime as discussed previously. A constant drag coefficient (n = 0) is used to represent the subsonic regime. The hybrid supersonic/subsonic model adds two additional parameters to model the drag behavior; the subsonic drag coefficient and the transition Mach number between subsonic and supersonic flight.

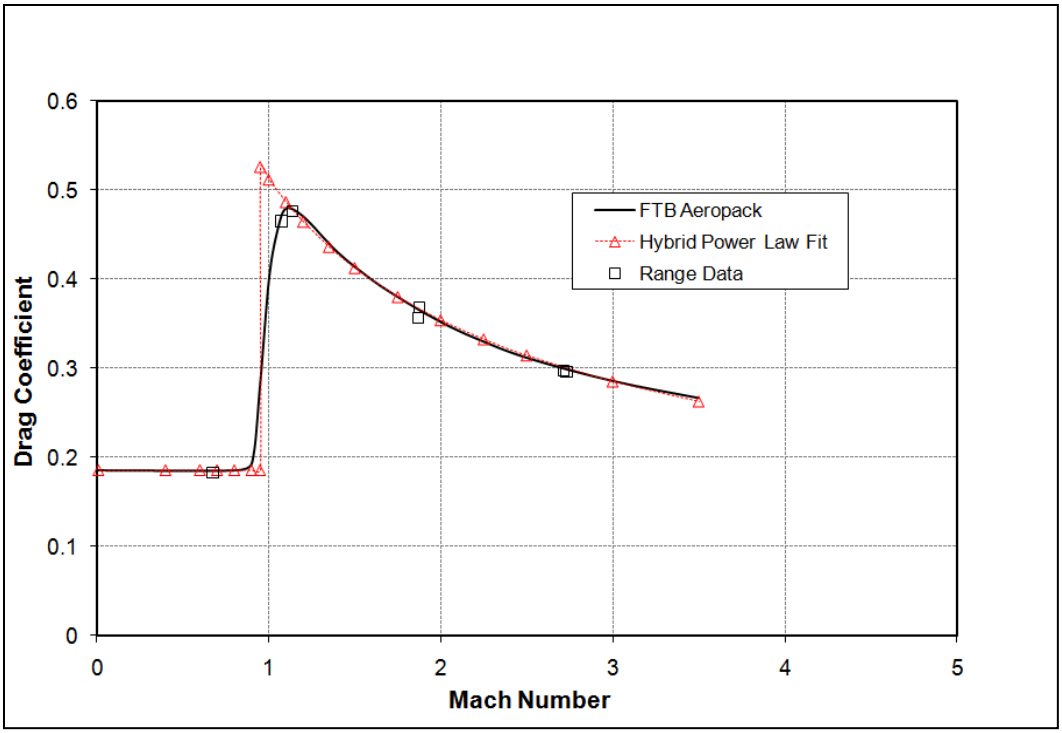

Figure 2. Hybrid supersonic/subsonic power-law drag coefficient model compared with aeropack and range data for the M855.

2.2 Analytical Solution Using A Hybrid Supersonic/Subsonic Power-Law Drag Model

For mixed supersonic/subsonic flight, the initial supersonic portion of the flight can be modeled using the analytical approach shown in reference 1. The analytical solutions are obtained using two main approximations. First, the gravity drop contributes little to total velocity during the flight. This assumption implies that the vertical displacement along the trajectory is small (direct-fire) and allows the 3DOF equations to be decoupled.

$$V = \sqrt{V_x^2 + V_y^2} \cong \overline{V}, \tag{11}$$

Secondly, the vertical and lateral displacements are small in relation to the downrange displacement and the total displacement along the trajectory (or slant-range) is nearly equal to the downrange displacement. This second assumption allows the downrange displacement to be treated as one of the primary independent variables.

$$s = \sqrt{s_x^2 + s_y^2 + s_z^2} \cong s_x, \tag{12}$$

2.2.1 Trajectory Model for Supersonic Portion of Flight

As shown in reference 1, using the power-law approach, analytical solution for the supersonic portion of flight can be obtained resulting in closed form equations for the dependent variables characterizing the projectile trajectory. These include the velocity V, time-of-flight t, gravity drop s_{g-drop}, vertical displacement of the projectile along the trajectory s_y and vertical deflection due to crosswind s_z as a function of range s_x. Equations 13–20 present closed-formed solutions for these dependent variables for a variable drag coefficient exponent ($n \neq 0,1,2$) as presented in reference 1; special case solutions for $n = 0, 1$ or 2 are also shown in reference 1. Inclusion of these solutions in the present analysis is straight-forward. The displacement due to wind drift in equation 17 is a classical crosswind drift formula based on the integration of the 3DOF equations as shown in reference 4.

$$V_x = \overline{V}\cos\theta_0, \tag{13}$$

$$V_y = \overline{V}\sin\theta_0 + V_{g-drop}, \tag{14}$$

$$\overline{V} = V_0\left\{1 + n\left(\frac{dV}{ds}\right)_0 \frac{s_x}{V_0}\right\}^{\frac{1}{n}}, \tag{15}$$

$$s_y = s_x \tan\theta_0 + s_{g-drop}, \tag{16}$$

$$s_z = w_z\left[t - \frac{s_x}{V_0}\right], \tag{17}$$

$$t = \frac{1}{(n-1)\left(\frac{dV}{ds}\right)_0}\left[\left\{1 + n\left(\frac{dV}{ds}\right)_0 \frac{s_x}{V_0}\right\}^{1-\frac{1}{n}} - 1\right], \tag{18}$$

$$s_{g-drop} = \frac{-g}{2(n-2)(n-1)\left(\frac{dV}{ds}\right)_0^2}\left[\left\{1 + n\left(\frac{dV}{ds}\right)_0 \frac{s_x}{V_0}\right\}^{\frac{2(n-1)}{n}} - 1 - 2(n-1)\left(\frac{dV}{ds}\right)_0 \frac{s_x}{V_0}\right], \tag{19}$$

$$V_{g-drop} = \frac{-g}{(n-2)\left(\frac{dV}{ds}\right)_0}\left[\left\{1 + n\left(\frac{dV}{ds}\right)_0 \frac{s_x}{V_0}\right\}^{\frac{n-1}{n}} - \left\{1 + n\left(\frac{dV}{ds}\right)_0 \frac{s_x}{V_0}\right\}^{\frac{1}{n}}\right], \quad n \neq 0,1,2 \tag{20}$$

Through the analysis, it can be shown that these trajectory characteristics are functions of only three primary variables, the projectile's muzzle velocity V_0, muzzle retardation $\left(\frac{dV}{ds}\right)_0$, and the exponent defining the shape of the drag curve, n. The trajectory is also a function of two independent parameters, the gravitational constant g, and the crosswind velocity w_z. The gun elevation angle θ_0 also appears in equations 13, 14, and 16 and can be treated as another independent parameter. However, the gun elevation angle θ_0 required to hit a target at range can be related to the three primary variables: the muzzle velocity, muzzle retardation, and drag coefficient exponent. In this regard, the gun elevation angle itself can be treated as a dependent variable. The muzzle velocity and muzzle retardation have the strongest influence on the trajectory and the exponent defining the shape of the drag curve can be shown to be a higher order effect whose influence is less important than the first two variables, particularly at shorter ranges.

The muzzle retardation is dependent on the projectile mass and muzzle drag coefficient as shown in equation 21.

$$\left(\frac{dV}{ds}\right)_0 = -\frac{1}{2m}\rho V_0 S_{ref} C_D\Big|_{V_0}, \tag{21}$$

Thus, the effect of both projectile mass and muzzle drag coefficient on the trajectory are represented by a single parameter—the muzzle retardation.

2.2.2 Transition Between Supersonic and Subsonic Flight

For the composite supersonic-subsonic model, equations 13–20 are valid until the projectile reaches the transition Mach number where the subsonic drag profile is used. The transition velocity is determined from the Mach number as shown in equation 22.

$$V_{tran} = a_\infty M_{tran} \tag{22}$$

Using equations 15 and 18–20, the range, time-of-flight, gravity drop, and gravity drop velocity where the transition occurs between the supersonic and subsonic drag profiles can be determined.

$$s_{x_{tran}} = \frac{1}{\left(\frac{dV}{ds}\right)_0 \frac{n}{V_0}}\left\{\left(\frac{V_{tran}}{V_0}\right)^n - 1\right\}, \tag{23}$$

$$t_{tran} = \frac{1}{(n-1)\left(\frac{dV}{ds}\right)_0}\left[\left\{1 + n\left(\frac{dV}{ds}\right)_0 \frac{s_{x\,tran}}{V_0}\right\}^{1-\frac{1}{n}} - 1\right], \tag{24}$$

$$s_{g-drop_{tran}} = \frac{-g}{2(n-2)(n-1)\left(\frac{dV}{ds}\right)_0^2}\left[\left\{1+n\left(\frac{dV}{ds}\right)_0 \frac{s_{x_{tran}}}{V_0}\right\}^{\frac{2(n-1)}{n}} -1-2(n-1)\left(\frac{dV}{ds}\right)_0 \frac{s_{x_{tran}}}{V_0}\right], \quad (25)$$

$$V_{g-drop_{tran}} = \frac{-g}{(n-2)\left(\frac{dV}{ds}\right)_0}\left[\left\{1+n\left(\frac{dV}{ds}\right)_0 \frac{s_{x_{tran}}}{V_0}\right\}^{\frac{n-1}{n}} -\left\{1+n\left(\frac{dV}{ds}\right)_0 \frac{s_{x_{tran}})}{V_0}\right\}^{\frac{1}{n}}\right] \quad (26)$$

2.2.3 Trajectory Model for Subsonic Portion of Flight

Using equations 23–26 as initial conditions, the governing 3DOF equations can be integrated to determine the trajectory in the subsonic portion of flight. The solution has a similar form to the solution for the supersonic portion of flight as shown in equations 27–30.

$$V_x = \overline{V}\cos\theta_0, \quad (27)$$

$$V_y = \overline{V}\sin\theta_0 + V_{g-drop}, \quad (28)$$

$$s_y = s_x \tan\theta_0 + s_{g-drop}, \quad (29)$$

$$s_z = w_z\left[t - \frac{s_x}{V_0}\right], \quad (30)$$

where,

$$\overline{V} = V_{tran}\exp\left\{\left(\frac{dV}{ds}\right)_{tran}\frac{(s_x - s_{x_{tran}})}{V_{tran}}\right\}, \quad (31)$$

$$t = t_{tran} + \frac{1}{\left(\frac{dV}{ds}\right)_{tran}}\left[1-\exp\left\{-\left(\frac{dV}{ds}\right)_{tran}\frac{(s_x - s_{x_{tran}})}{V_{tran}}\right\}\right], \quad (32)$$

$$s_{g-drop} = \frac{-g}{4\left(\frac{dV}{ds}\right)_{tran}^2}\left(2\left(\frac{dV}{ds}\right)_{tran}\frac{(s_x - s_{x_{tran}})}{V_{tran}} + \exp\left\{-2\left(\frac{dV}{ds}\right)_{tran}\frac{(s_x - s_{x_{tran}})}{V_{tran}}\right\} - 1\right), + \frac{V_{g-drop_{tran}}}{V_{tran}}(s_x - s_{x_{tran}}) + s_{g-drop_{tran}} \quad (33)$$

$$V_{g-drop} = \frac{-g}{2\left(\frac{dV}{ds}\right)_{tran}}\left[\exp\left(\left(\frac{dV}{ds}\right)_{tran}\frac{(s_x - s_{x_{tran}})}{V_{tran}}\right) - \exp\left(-\left(\frac{dV}{ds}\right)_{tran}\frac{(s_x - s_{x_{tran}})}{V_{tran}}\right)\right], \quad (34)$$
$$+V_{g-drop_{tran}}\exp\left(\left(\frac{dV}{ds}\right)_{tran}\frac{(s_x - s_{x_{tran}})}{V_{tran}}\right)$$

Here the retardation at the transition point is determined from equation 35.

$$\left(\frac{dV}{ds}\right)_{tran} = -\frac{1}{2m}\rho V_{tran} S_{ref} C_D\Big|_{V_{tran}} . \quad (35)$$

The composite solution for supersonic and subsonic trajectories adds two additional parameters (transition Mach number and retardation or drag coefficient at the transition Mach number) to the three parameters (muzzle velocity, muzzle retardation, and drag coefficient exponent) in the original power-law approach. Using these five parameters, the trajectory from supersonic to subsonic flight can be determined using closed-form expressions that are very easy to implement.

2.2.4 Sources of Approximation or Uncertainty in the Current Approach

There are two notable sources of approximation or uncertainty in applying the approach of power-law methodology. The first uncertainty is associated with the approximation made to obtain closed form analytical solution of the point-mass trajectory equations. This approximation assumes that the component of velocity produced by gravity is small and can be ignored when computing the aerodynamic drag of the projectile. This approximation is valid for flat fire and has been shown to produce very little error when compared with more exact numerical solutions of the governing equations.

The second source of error is associated with modeling the variation of the drag coefficient with Mach number using a power-law approach. The power-law approach represents a very useful method for conceptual design because its simplicity and physical accuracy in representing the drag variation with Mach number whether analytical or numerical solutions of the point-mass equations are sought. The analysis of reference 1 shows that the supersonic drag variation of a wide variety of munitions can be accurately modeled using this approach. Furthermore, the predicted trajectories obtained using this approach show surprisingly little sensitivity to the exponent used in the power-law formulation. This implies that the shape of the drag curve is not a dominant factor in predicting the trajectory, particularly when compared with the muzzle velocity and muzzle retardation. This is significant because when the current approach is used in a conceptual design approach, the design process can focus on muzzle velocity and muzzle retardation as the significant design variables defining the point-mass trajectories.

The extension of the power-law approach to flight regimes that include supersonic and subsonic flight introduces additional degrees of freedom in the drag variability through the addition of the

subsonic drag coefficient and the transition Mach number. For many munitions, the drag is essentially constant in the subsonic regime and its uncertainty is related to the predictive or measurement accuracies. On the other hand, the transition Mach number is directly associated with the power-law method and the uncertainty of the results to its selection is perhaps less well understood. This uncertainty is addressed further in the results section.

3. Results

The hybrid subsonic/supersonic trajectory model is applied here in two example applications to demonstrate the performance of the method. Results are shown first for the 5.56-mm M855 projectile fired from the M16 rifle. The flight of the M855 projectile occurs at supersonic velocities over its useful operational range. However, there may be instances where trajectory information may be required at longer ranges where the flight velocity drop below the sonic velocity. Results are also shown for a 9-mm pistol bullet, which is typically launched at supersonic velocities and may reach subsonic velocities later in flight. For both of these examples, the supersonic power-law model is no longer valid once the projectile reaches subsonic velocities and alternative approach such as the hybrid supersonic/subsonic model must be applied.

3.1 Results for the 5.56-mm M855

Trajectory results for the 5.56-mm M855 fired from the M16 rifle were generated using the hybrid supersonic/subsonic model. Table 1 shows the parameters used in the model. Parameters were evaluated at standard atmospheric conditions. Comparisons were also made with trajectory predictions made with the 4DOF model within Prodas (*7*) using the FTB aeropack data (*5*).

Table 1. Parameters for M855 projectile used in hybrid supersonic/subsonic model.

Muzzle velocity, V_0	949 m/s
Muzzle retardation, $\left(\frac{dV}{ds}\right)_0$	–1.064 (m/s)/m
Drag coefficient exponent, n	0.53
Transition mach number, M_{tran}	0.95
Subsonic retardation at M_{tran}, $\left(\frac{dV}{ds}\right)_{tran}$	–0.2421 (m/s)/m

Figure 3 shows the predicted velocity as a function of range. The velocity of the projectile remains above the sonic velocity until about 700 m of flight. Within the first 700 m of flight, the supersonic power-law model produces excellent agreement with the Prodas prediction. Beyond 700 m, the velocity of the projectile drops below the sonic velocity and the projectile enters a region of lower-drag subsonic flight as evidenced by the decreased velocity fall-off. The predictions of the hybrid supersonic/subsonic model provide excellent agreement with the Prodas prediction across both the supersonic and subsonic regions of flight. Extrapolation of the supersonic power-law model into the subsonic region provides increasingly worse results as the range increases. Here, the power-law drag model predicts exponentially increasing drag as the velocity approaches zero compared with a constant drag that is typically observed in the subsonic regime.

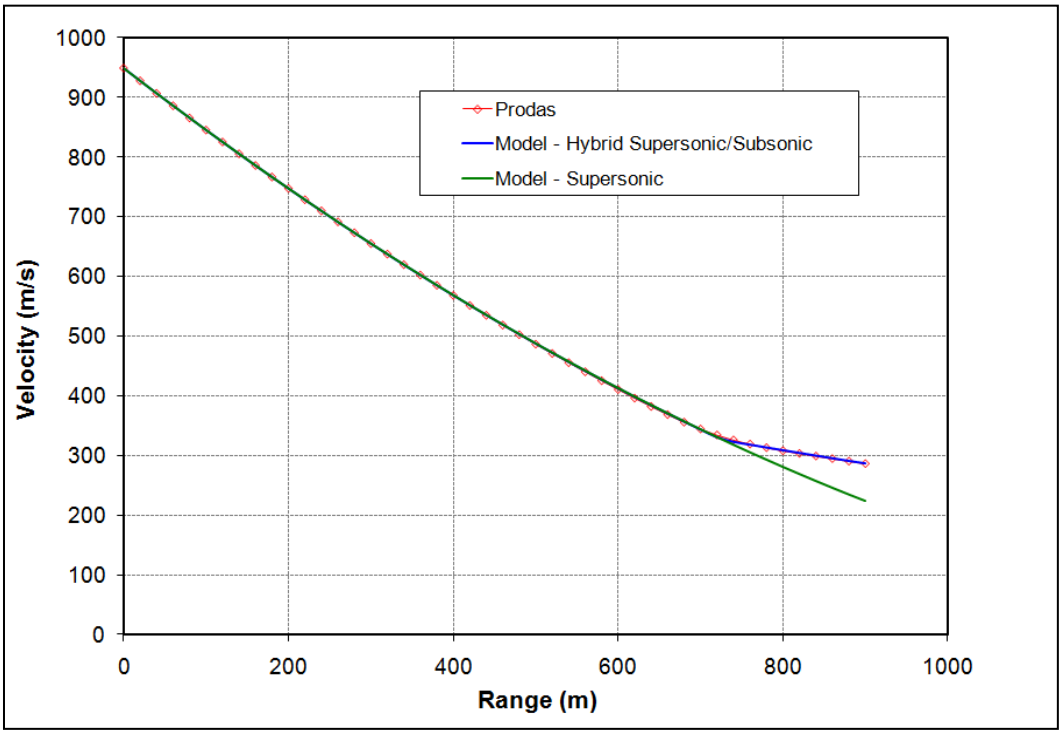

Figure 3. Velocity as a function of range, M855.

Figures 4–6 show the predicted time-of-flight, the gravity drop and the wind drift as a function of range. Within the supersonic regime, the results show excellent agreement between the supersonic power-law model and Prodas. However, once the projectile reaches subsonic velocities, the errors in the supersonic model become apparent. In the subsonic region, the hybrid supersonic/subsonic model provides excellent agreement with the Prodas predictions.

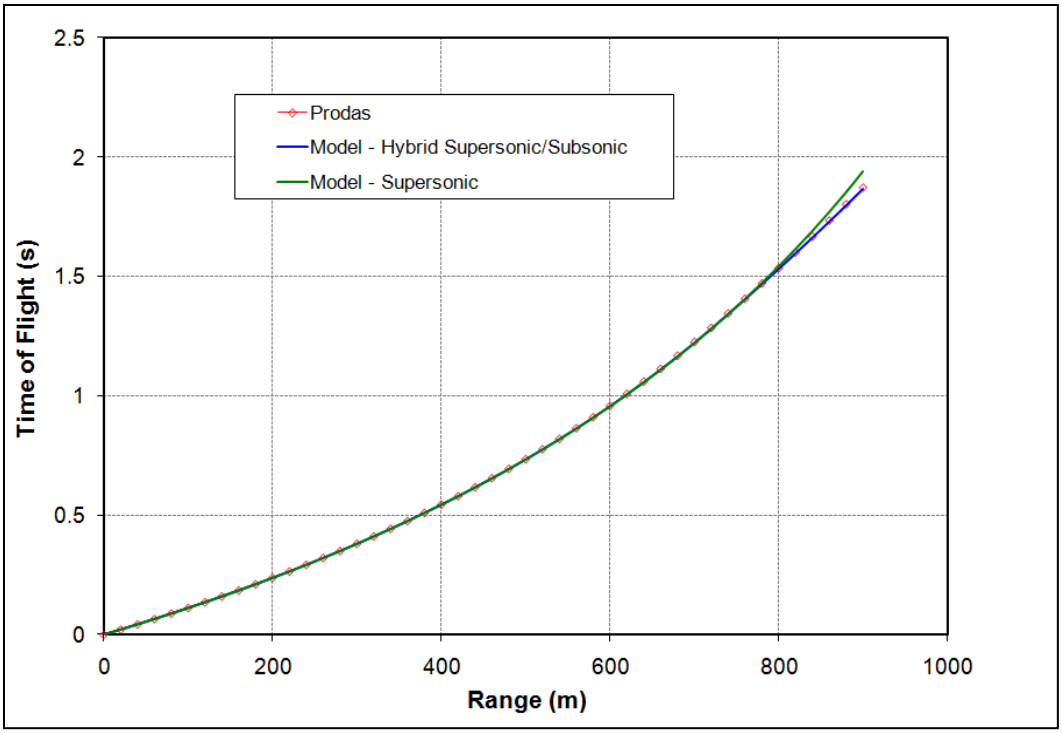

Figure 4. Time-of-flight vs. range, M855.

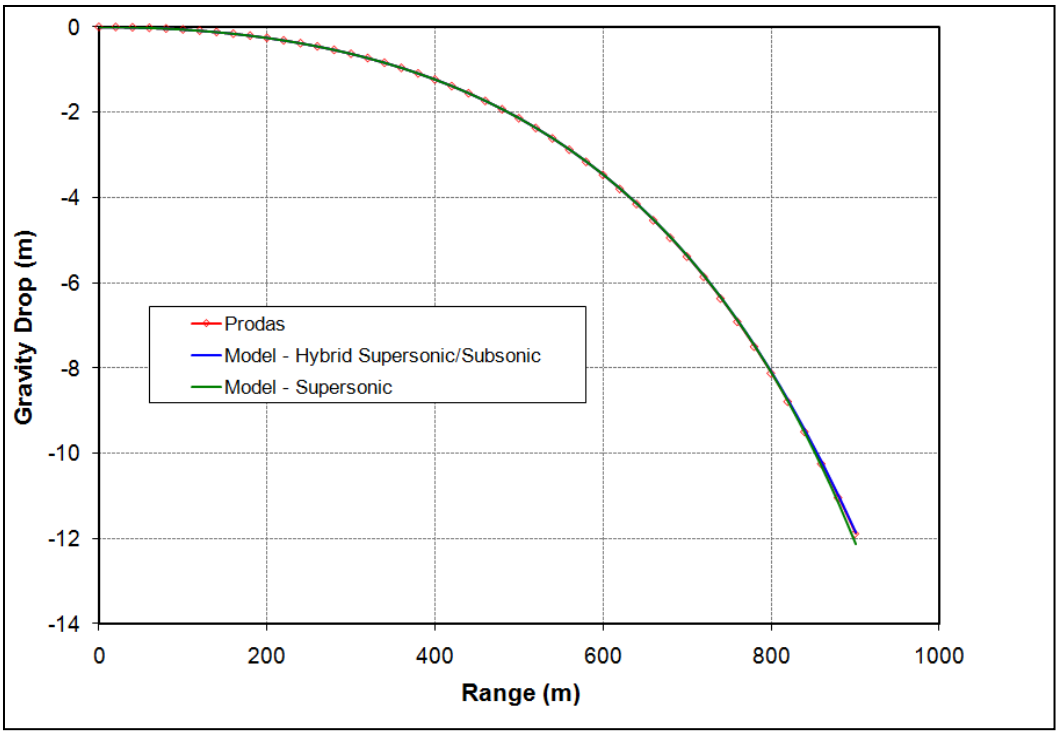

Figure 5. Gravity drop vs. range, M855.

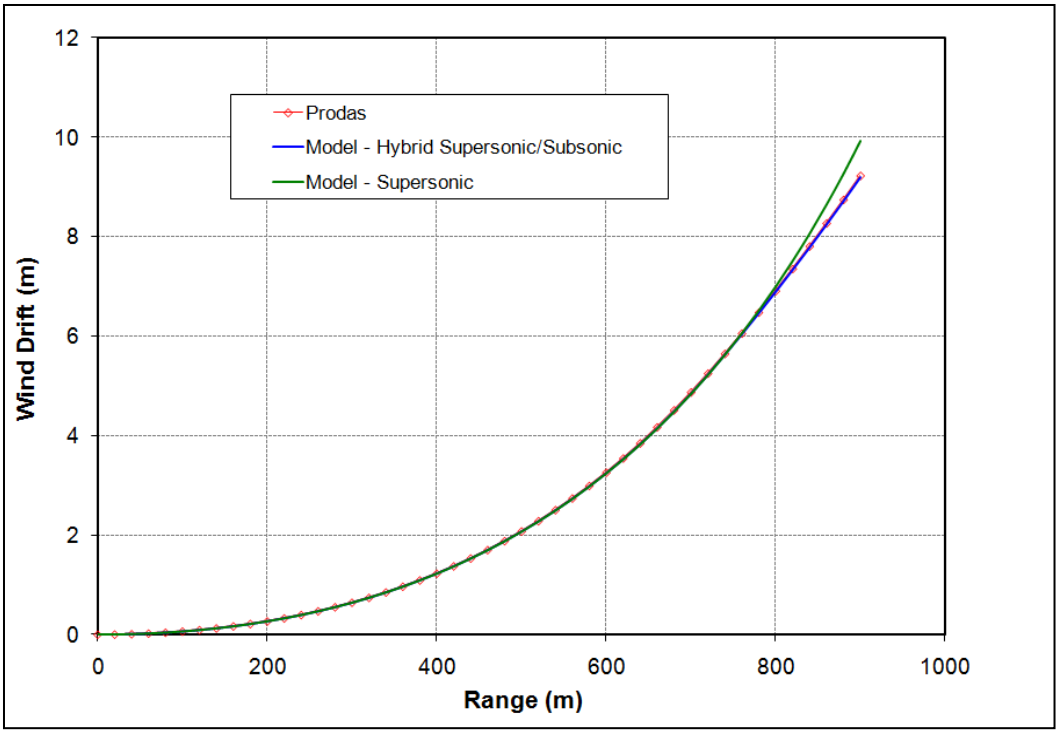

Figure 6. Wind drift vs. range, M855.

Relatively speaking, the differences between the hybrid supersonic/subsonic method and the supersonic methods for these three quantities are less than the differences observed for the velocity seen previously in figure 3. This is because these quantities are essentially integrated effects of the velocity that includes a significant portion of supersonic flight. Extrapolation of these quantities into the high subsonic regime using the supersonic power-law method may provide a reasonable approximation to the actual behavior. However, the extrapolation rapidly falls apart due to the exponentially increasing drag as the velocity approaches zero.

Figure 7 shows the predicted gravity drop velocity as a function of range. Excellent agreement between the hybrid supersonic/subsonic model and the Prodas predictions are seen. Significant discrepancies between the supersonic power-law model and the other two approaches are seen once the projectile reaches subsonic velocities. Although not normally considered a dependent variable of significant interest, the gravity drop velocity at the transition velocity is required as an initial condition for the integration of the vertical displacement. Figure 7 provides validation of the analytical results for the gravity drop velocity in both the supersonic and subsonic regime.

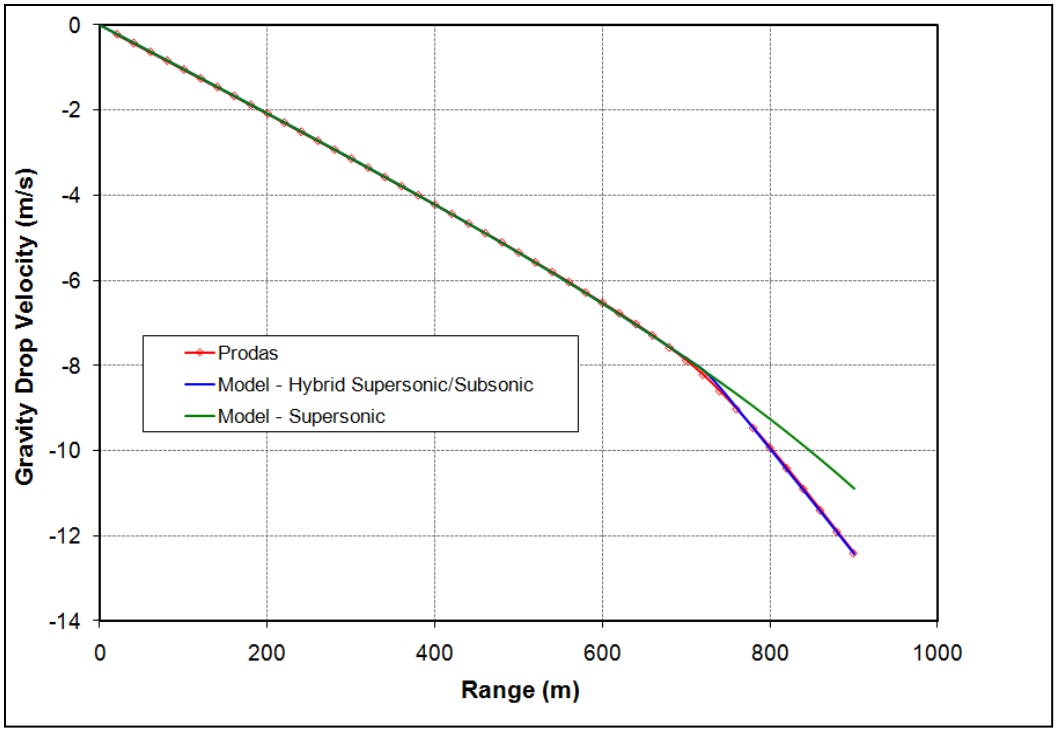

Figure 7. Gravity drop velocity vs. range, M855.

3.2 Results for the 9-mm Ball Pistol Bullet

Trajectory results for the 9-mm ball projectile fired from a 9-mm pistol were generated using the hybrid supersonic/subsonic model. Table 2 shows the parameters used in the model. Parameters were evaluated at standard atmospheric conditions. Comparisons were also made with trajectory predictions made with the 4DOF model within Prodas (*7*) using an existing drag profile shown in figure 8. Also shown in figure 8 is the drag variation used in the hybrid supersonic/subsonic power law model.

Table 2. Parameters for 9-mm ball projectile used in hybrid supersonic/subsonic model.

Muzzle velocity, V_0	416 m/s
Muzzle retardation, $\left(\frac{dV}{ds}\right)_0$	–1.74 (m/s)/m
Drag coefficient exponent, n	0.27
Transition mach number, M_{tran}	0.925
Subsonic retardation at M_{tran}, $\left(\frac{dV}{ds}\right)_{tran}$	–0.4612 (m/s)/m

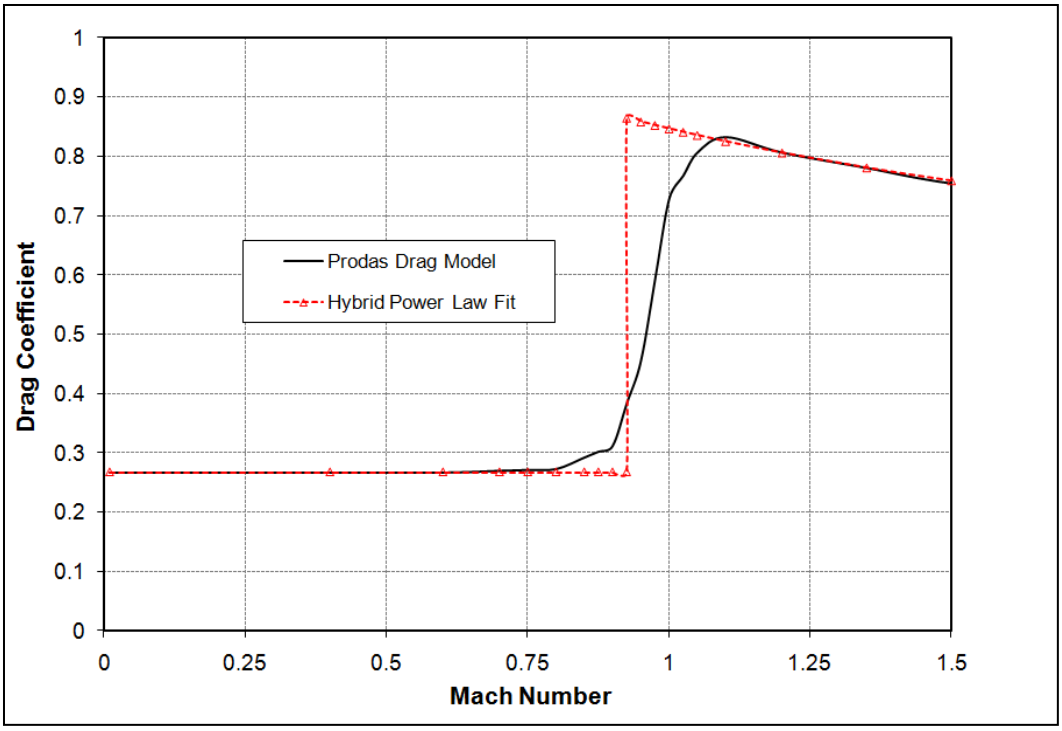

Figure 8. Drag coefficient as a function of Mach number, 9-mm pistol bullet.

Figure 9 shows the predicted velocity as a function of range obtained with the supersonic/subsonic model compared with Prodas predictions and the supersonic power-law model. Each of the models shows excellent agreement from launch to the sonic velocity (340 m/s). It should be noted that for the current application, the results are relatively insensitive to the drag coefficient exponent (for the supersonic drag power-law) because the supersonic portion of flight is relatively short. The supersonic/subsonic model shows an abrupt change in the velocity fall-off as the model transitions from the supersonic regime to the subsonic regime. The Prodas model, on the other hand, shows a gradual change in the velocity fall-off through the transonic regime because the model more properly accounts for the drag variation in the transonic regime. Both the supersonic/subsonic model and the Prodas predictions show similar velocity variations in the subsonic regime where the drag coefficient is constant.

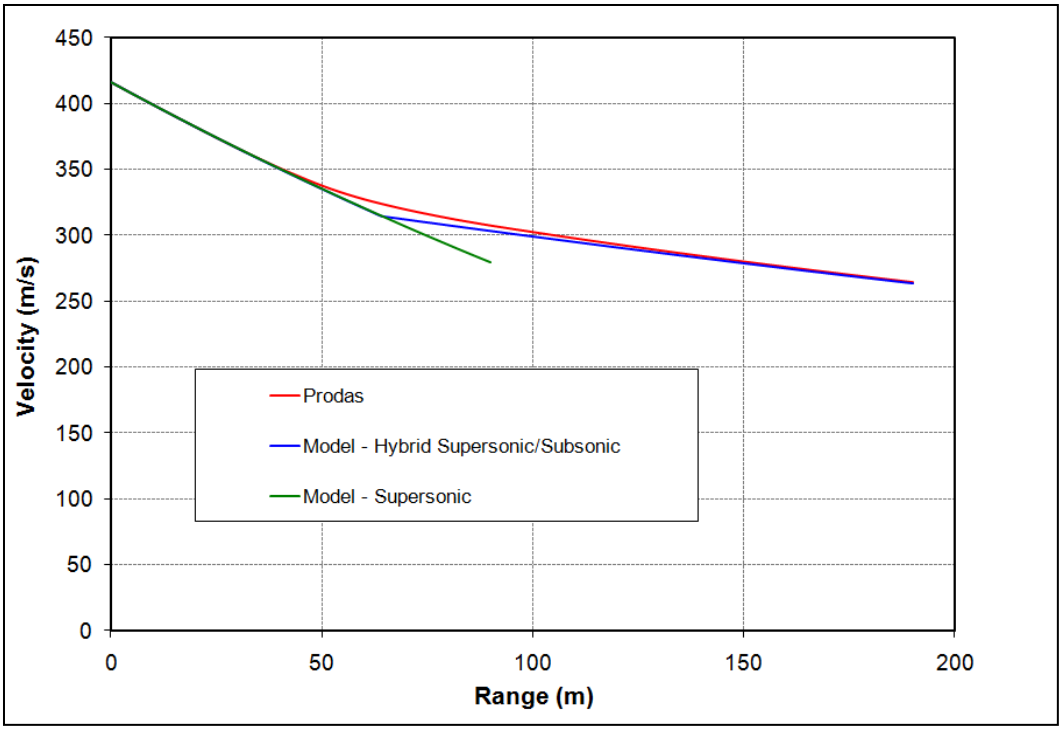

Figure 9. Velocity as a function of range, 9-mm pistol bullet.

Figures 10–12 show the predicted time-of-flight, the gravity drop and the wind drift as a function of range. The hybrid supersonic/subsonic model shows excellent agreement with the Prodas predictions for these quantities. The small discrepancies between the hybrid supersonic/subsonic model and the Prodas prediction are due to the fact that the supersonic/subsonic model does not account for the drag variation in the transonic regime and abruptly transitions the drag coefficient between supersonic and subsonic flight.

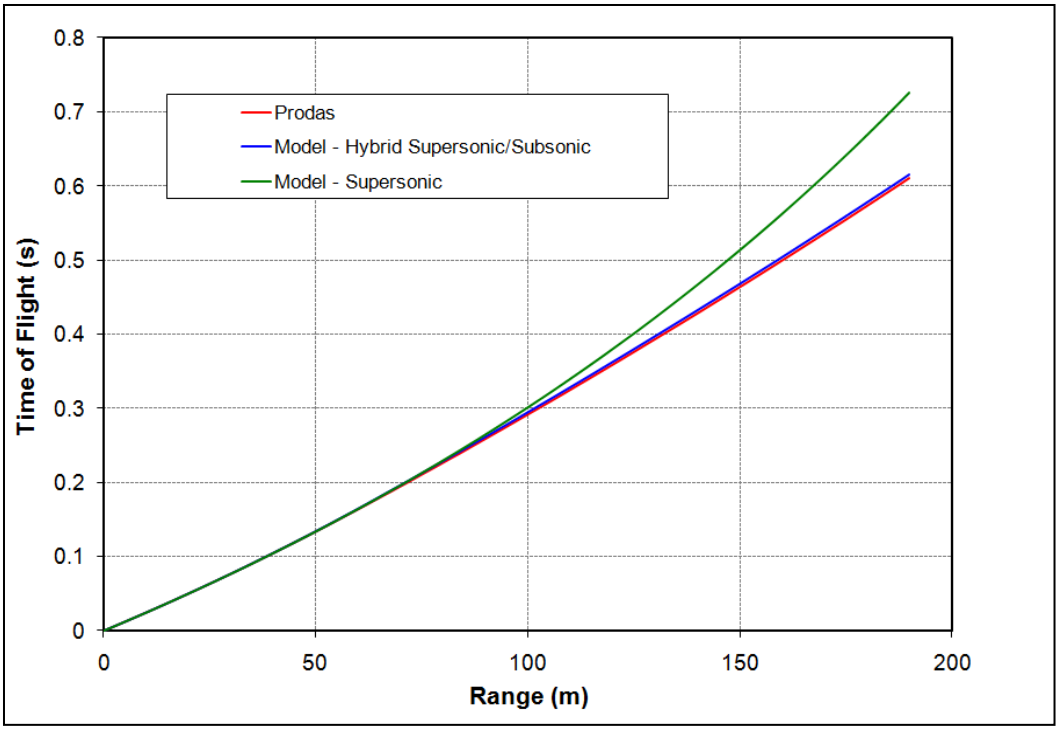

Figure 10. Time-of-flight vs. range, 9-mm pistol bullet.

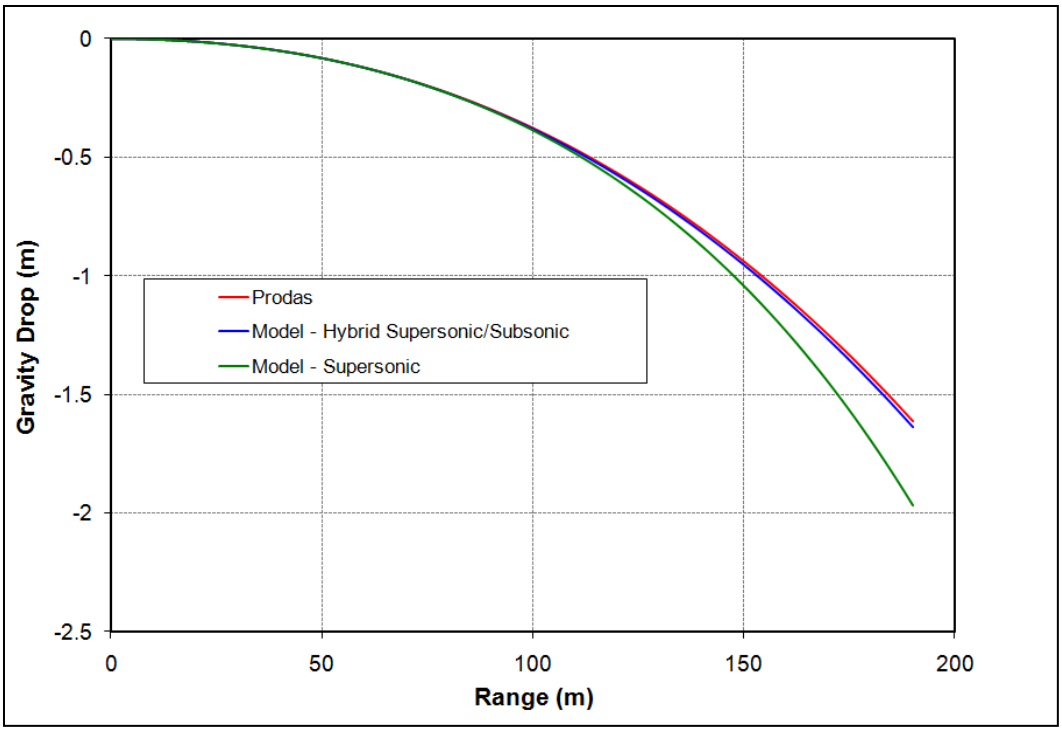

Figure 11. Gravity drop vs. range, 9-mm pistol bullet.

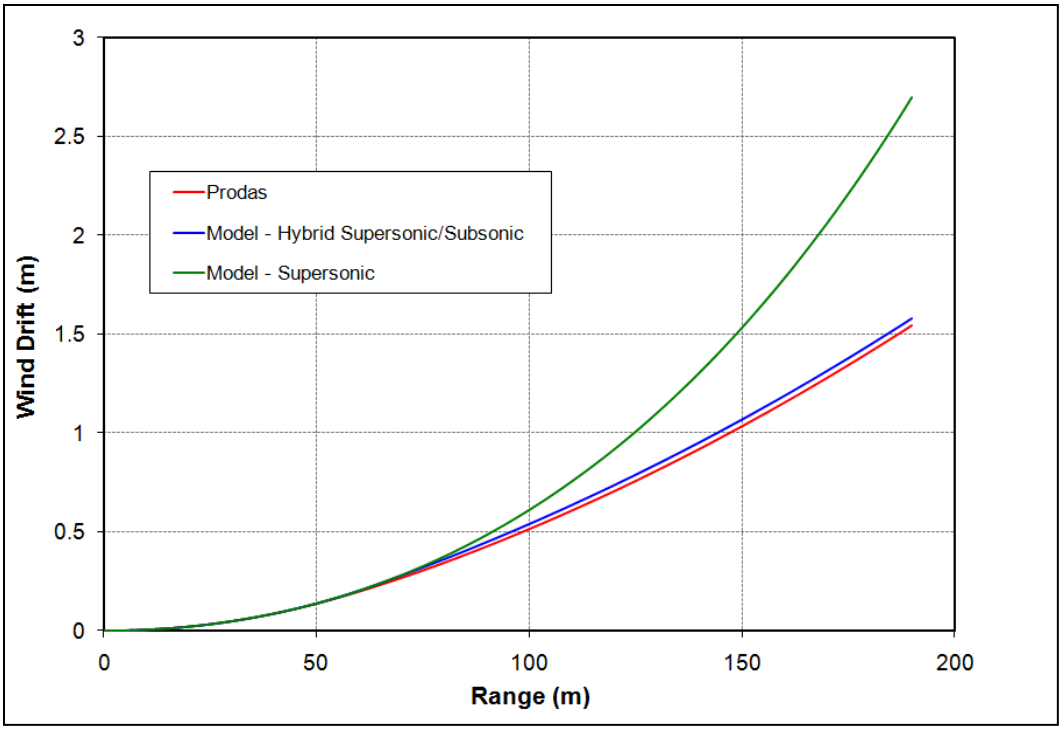

Figure 12. Wind drift vs. range, 9-mm pistol bullet.

Figure 13 shows the gravity drop velocity as a function of range. In the supersonic regime, the supersonic power-law approach shows excellent agreement with the Prodas predictions. Once reaching the sonic velocity, the hybrid method shows better agreement with the Prodas predictions than does the extrapolation of the supersonic power-law model into the subsonic regime. Like the results shown in figures 10–12, the discrepancy between the hybrid supersonic/subsonic model and the Prodas predictions is due to the treatment of the drag coefficient within both models in the transonic regime.

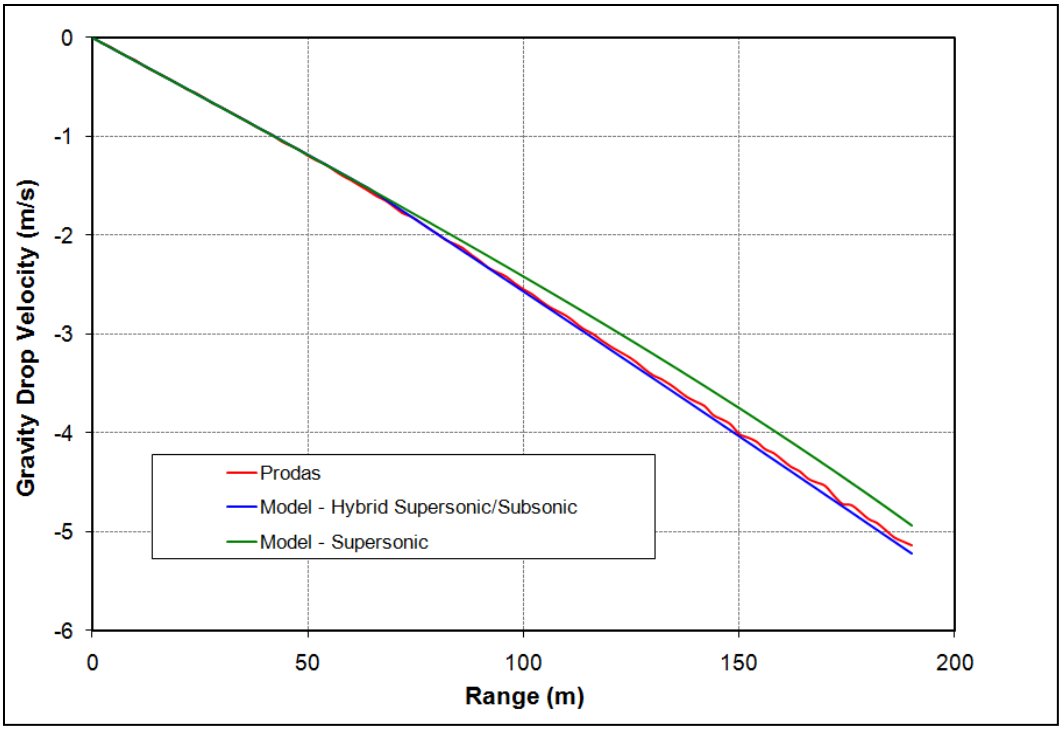

Figure 13. Gravity drop velocity vs. range, 9-mm pistol bullet.

In addition to the three parameters (muzzle velocity, muzzle retardation, and drag coefficient exponent) required for the supersonic power-law model, the hybrid supersonic/subsonic model requires two additional parameters to model the subsonic portion of flight; the transition Mach number and the subsonic retardation at the transition Mach number (essentially, the subsonic drag coefficient). Since the current analysis focuses on the performance of the trajectory prediction method, the hybrid supersonic/subsonic method assumes that the physical and aerodynamic characteristics of the round needed to determine muzzle velocity, muzzle and transition retardations and drag coefficient exponents are provided by auxiliary methods. These include engineering design codes like Prodas or engineering design approaches such as those presented in reference 2, for small caliber rifle bullets.

However, the determination of the transition Mach number is not so straight-forward. If a reference velocity history is available, the transition Mach number can be tailored so that the hybrid supersonic/subsonic model provides the same velocity history in the subsonic regime as the reference trajectory. While it can be argued that the existence of the velocity history might indicate that an alternative method of trajectory prediction is redundant, there are examples where a simplified trajectory method is still beneficial. For example, in performance assessment codes where large numbers of trajectories are required, a simplified model based on a reference trajectory provides an efficient method in lieu of a more complex numerical solution.

Additionally, some experimental methods, such as radar tracking may provide velocity history information which can be translated into accurate trajectory displacement data (gravity drop, wind drift) using the current power-law methods.

The sensitivity of the results to the transition Mach number was also examined in the current study. The transonic regime is generally considered to occur between Mach 0.8 and 1.2, with most of the transonic drag rise occurring between Mach 0.9 and Mach 1.0. Thus, the transition Mach number should be within this range. Figure 14 shows the velocity as a function of range. Results using the hybrid supersonic/subsonic method are shown with three different transitions Mach numbers; 0.9, 0.925 and 0.95. As shown in table 2, Mach 0.925 represents the transition Mach number used to obtain the baseline results shown previously in figures 9–13. In the results shown here, the transition retardation has been adjusted for velocity using equation 36.

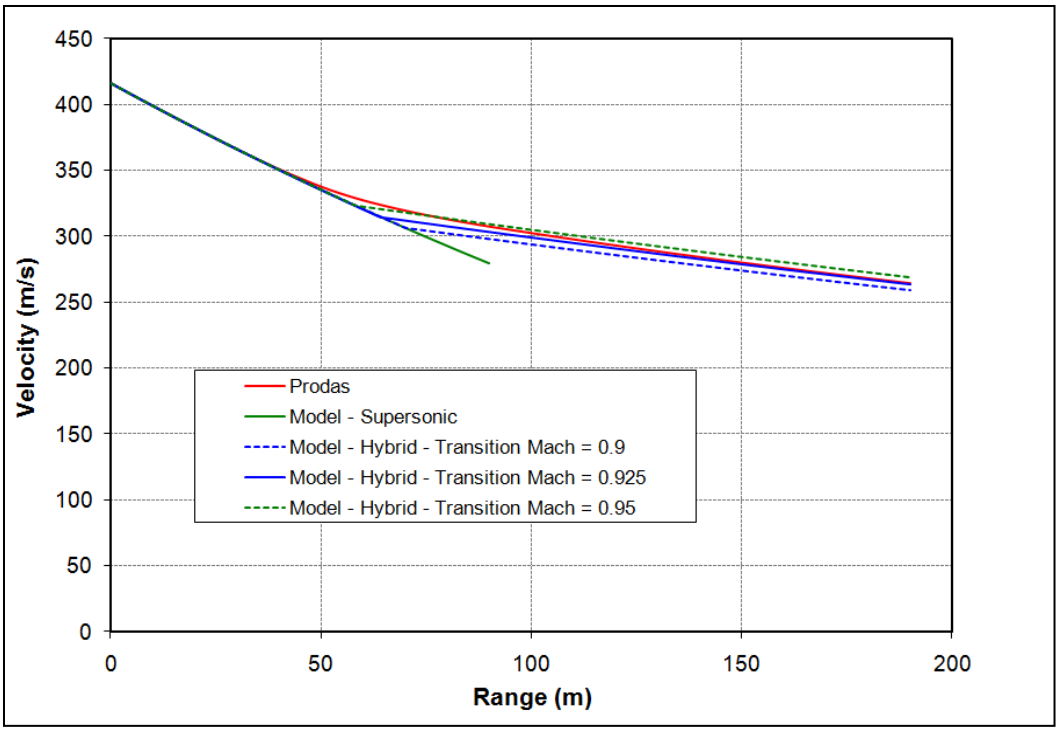

Figure 14. Sensitivity of velocity vs. range to selection of transition Mach number, 9-mm pistol bullet.

$$\left(\frac{dV}{ds}\right)_{new} = \left(\frac{V_{new}}{V_{baseline}}\right)^{1-n} \left(\frac{dV}{ds}\right)_{baseline}. \tag{36}$$

The results show that the higher transition Mach number of 0.95 produces an over-prediction of the velocity in the subsonic regime while the lower transition Mach number of 0.9 produces an under-prediction of the velocity compared with the Prodas results. The differences are relatively constant with range and on the order of a couple of percent.

Figures 15–17 show the sensitivity of the predicted time-of-flight, the gravity drop and the wind drift to the transition Mach number. The sensitivity of the results are less than 2% for the time-of-flight and the gravity drop and less than 5% for the wind drift. These results show that the results are relatively insensitive to the transition Mach number.

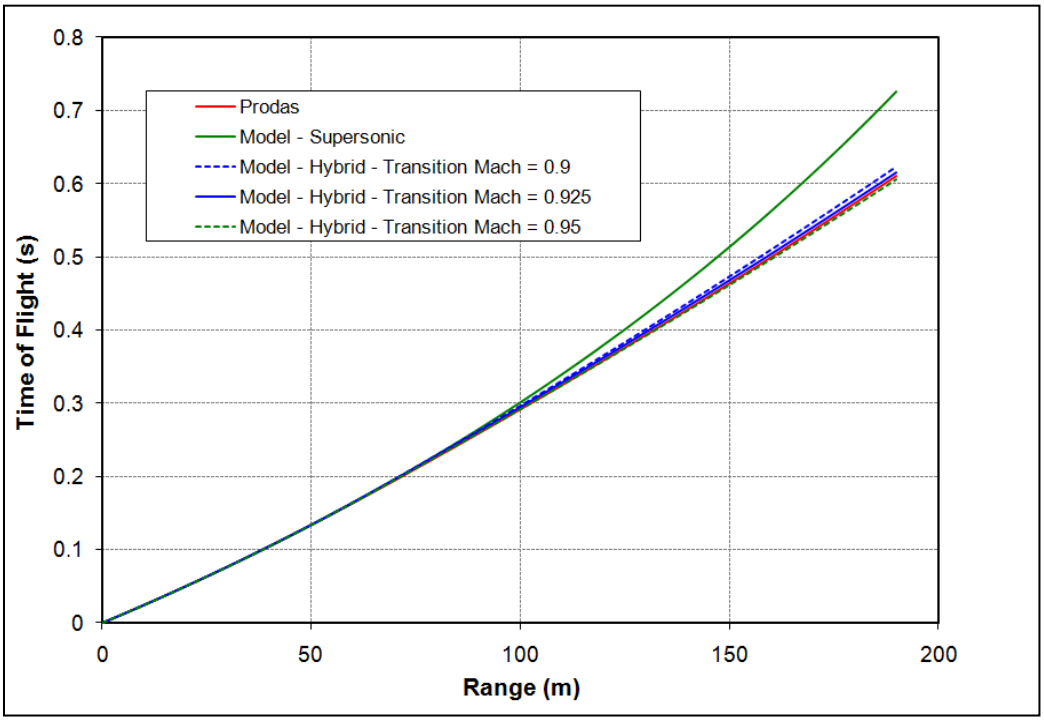

Figure 15. Sensitivity of time-of-flight vs. range to selection of transition Mach number, 9-mm pistol bullet.

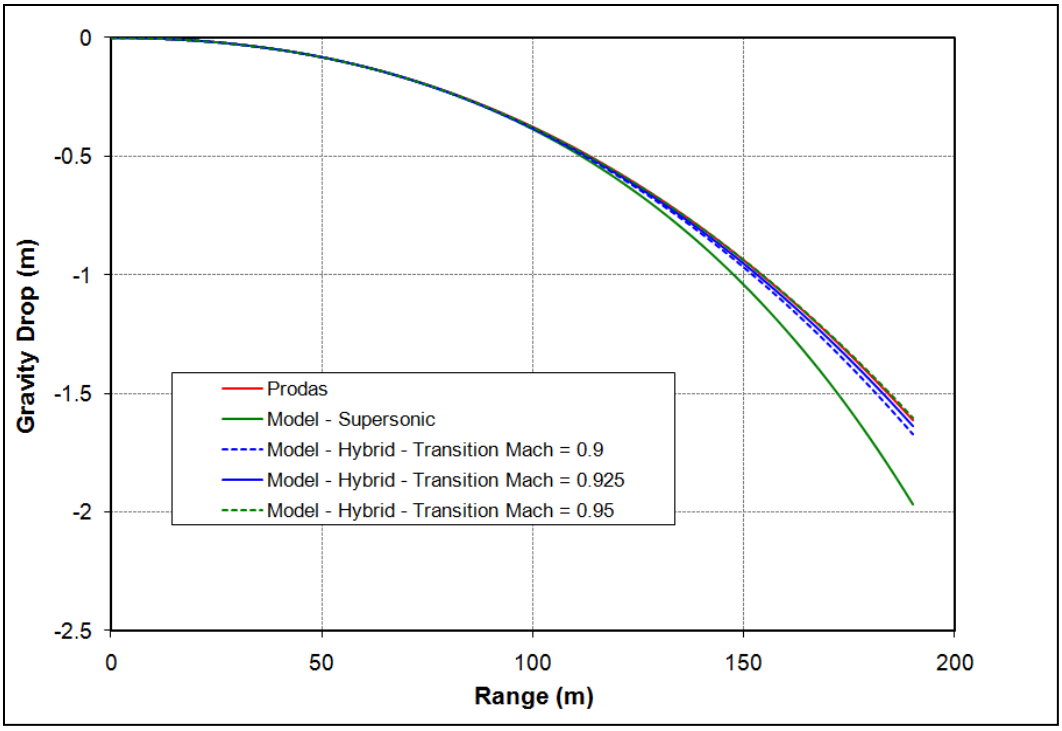

Figure 16. Sensitivity of gravity drop vs. range to selection of transition Mach number, 9-mm pistol bullet.

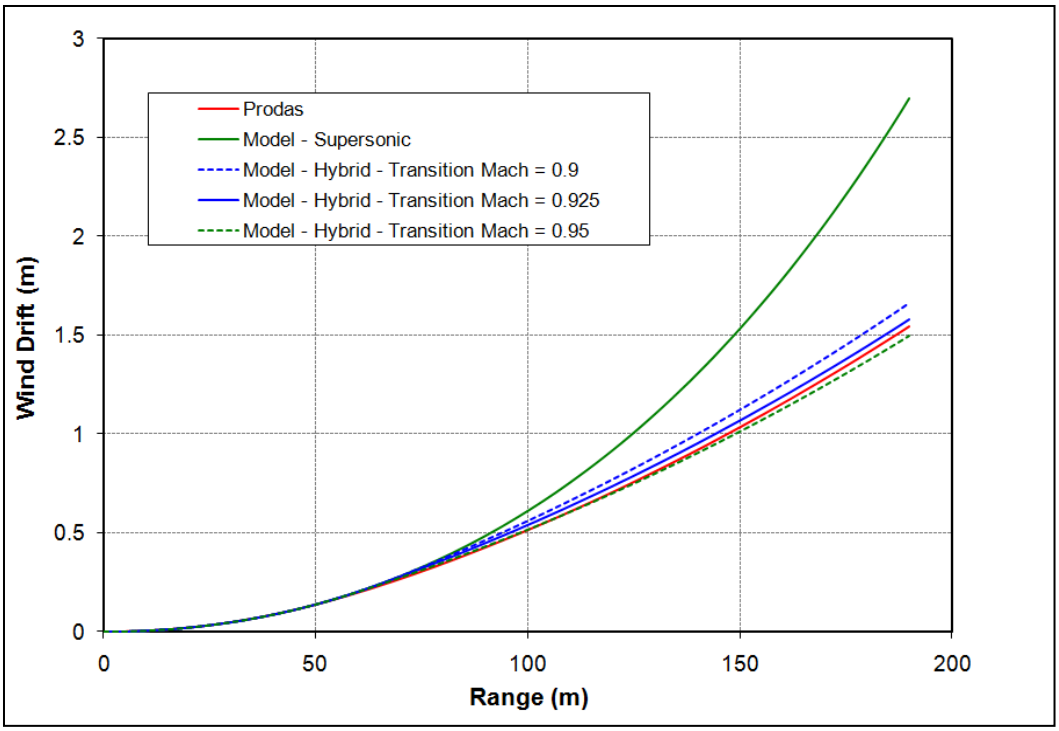

Figure 17. Sensitivity of wind drift vs. range to selection of transition Mach number, 9-mm pistol bullet.

When discussing the sensitivity of the results to the selection of the transition Mach number it is important to understand that the transonic drag behavior is often not completely characterized and therefore is a subject of some uncertainty itself. For many projectiles, the transonic regime may not be of significant enough interest to warrant complete characterization of the aerodynamics. Often, an assumed form for transonic drag rise is used, which introduces its own uncertainty in the trajectory prediction. As shown in the results presented here, this assumption may only produce minor differences in the predicted trajectory. Thus, consideration of the uncertainty produced by the selection of the transition Mach number must be balanced by the actual uncertainty that may exist in the transonic drag behavior of the projectile.

4. Conclusion

An approach for predicting the trajectory of projectiles with mixed supersonic and subsonic flight is presented. The analysis presented shows that projectile flight with mixed supersonic and subsonic flight can be predicted with five parameters; the muzzle velocity, the muzzle retardation, a power-law exponent that describes the shape of the drag curve is supersonic flight, the transition Mach number between supersonic and subsonic portions of flight, and the subsonic retardation at the transition Mach number (or alternatively the subsonic drag coefficient). Closed-form expressions for the velocity, time-of-flight, gravity drop and wind drift are developed to provide critical information about the trajectory of projectiles in direct-fire (low gun elevation angles).

The power of the method is two-fold. First, the method allows accurate prediction of direct-fire trajectories using simple closed-form expressions. These types of expressions are particularly useful for design studies or performance assessment studies where there is a need for rapid prediction of trajectories and are much easier to implement compared with numerical trajectory prediction methods. Second, the method distills the trajectory description down to a small number of parameters that, along with knowledge of their relative sensitivities, allows a better technical understanding of the parameters that drive the characteristics of the trajectory.

The method is shown to accurately predict trajectories when compared with four degree-of-freedom numerical trajectory predictions. The current method, which assumes an abrupt transition between supersonic and subsonic flight, does not consider the details of the transonic portion of flight. However, the results seem to show relatively small effects of this assumption for the applications examined here. The results shown here also show the relative errors that can be present if the previous supersonic method is simply extrapolated into the subsonic regime. The current method overcomes these issues and allows a more appropriate modeling of the trajectory once the projectile reaches subsonic flight.

In previous studies (*1*, *2*), for the supersonic portion of flight, the trajectory was shown to be most sensitive to the muzzle velocity and muzzle retardation. The power-law exponent describing the shape of the drag curve was shown to be a less sensitive parameter. Once the projectile reaches subsonic flight, the current study shows that the subsonic retardation is a more sensitive parameter compared with the transition Mach number.

The method is currently being applied in design studies for concepts that span both supersonic and subsonic regimes. This method allows a more complete and accurate assessment of a wider range of projectile concepts than was possible with the previous power-law method that was limited to supersonic flight.

5. References

1. Weinacht, P.; Cooper, G. R.; Newill, J. F. *Analytical Prediction of Trajectories for High-Velocity Direct-Fire Munitions*; ARL-TR-3567; U.S. Army Research Laboratory: Aberdeen Proving Ground, MD, 2005.

2. Weinacht, P.; Newill, J. F.; Conroy, P. J. *Conceptual Design Approach for Small-Caliber Aeroballistics with Application to 5.56-mm Ammunition*; ARL-TR-3620; U.S. Army Research Laboratory: Aberdeen Proving Ground, MD; 2005.

3. McCoy, R. L. *Modern Exterior Ballistics*; Schiffer Military History: Atglen, PA, 1999.

4. McCoy, R. L. *The Effect of Wind on Flat-Fire Trajectories*; BRL Report No. 1900, U.S. Army Ballistic Research Laboratories: Aberdeen Proving Ground, MD, 1976.

5. Tilghman, B. A. Firing Tables Branch, U.S. Army Armament RD&E Center, Aberdeen Proving Ground, MD. Private Communication on M855 Aeropack Data, 2003.

6. McCoy, R. L. *Aerodynamic and Flight Dynamic Characteristics of the New Family of 5.56 mm NATO Ammunition*; BRL-MR-3476, U.S. Army Ballistics Research Laboratory: Aberdeen Proving Ground, MD, 1985.

7. Anonymous. *Prodas Users Manual*; Arrow Tech Associates: Burlington, VT, 2002.

6. Glossary

C_D	Drag coefficient
$C_D\|_{V_0}$	Drag coefficient evaluated at the muzzle velocity
$C_D\|_{V_{tran}}$	Drag coefficient evaluated at the transition velocity between supersonic and subsonic flight
D	Reference diameter
g	Gravitational acceleration
m	Projectile mass
M	Mach number
M_{tran}	Mach number at transition between supersonic and subsonic flight
n	Exponent defining shape of the drag versus Mach number curve
s	Total downrange displacement
s_{g-drop}	Gravity drop
$s_{g-drop_{tran}}$	Gravity drop evaluated at the transition between supersonic and subsonic flight
s_x, s_y	Horizontal and vertical displacement along trajectory
$s_{x_{tran}}$	Horizontal (downrange) displacement where transition between supersonic and subsonic flight occurs
s_z	Out-of-plane displacement along trajectory (normal to x-y plane)
S_{ref}	Reference area, $S_{ref} = \frac{\pi D^2}{4}$
t	Time-of-flight
t_{tran}	Time where transition between supersonic and subsonic flight occurs
V	Total velocity
V_0	Muzzle velocity

$V_{Baseline}$ Baseline velocity used in adjusting retardation for velocity changes

V_{New} New velocity used in adjusting retardation for velocity changes

V_{g-drop} Vertical velocity component due to gravity

$V_{g-drop_{tran}}$ Vertical velocity component due to gravity evaluate at the transition between supersonic and subsonic flight

V_{tran} Transition velocity between supersonic and subsonic flight

V_x, V_y Downrange and vertical velocity components, respectively

$\left(\frac{dV}{ds}\right)_0$ Muzzle retardation

$\left(\frac{dV}{ds}\right)_{Baseline}$ Baseline retardation used in adjusting retardation for velocity changes

$\left(\frac{dV}{ds}\right)_{New}$ Retardation adjusted for velocity changes

$\left(\frac{dV}{ds}\right)_{tran}$ Retardation evaluated at transition velocity between supersonic and subsonic flight

w_z Crosswind velocity

Greek Symbols

θ_0 Initial gun elevation angle

ρ Atmospheric density

NO. OF
COPIES ORGANIZATION

1 (PDF only) DEFENSE TECHNICAL INFORMATION CTR
DTIC OCA
8725 JOHN J KINGMAN RD
STE 0944
FORT BELVOIR VA 22060-6218

1 DIRECTOR
US ARMY RESEARCH LAB
IMNE ALC HRR
2800 POWDER MILL RD
ADELPHI MD 20783-1197

1 DIRECTOR
US ARMY RESEARCH LAB
RDRL CIO LL
2800 POWDER MILL RD
ADELPHI MD 20783-1197

1 DIRECTOR
US ARMY RESEARCH LAB
RDRL CIO MT
2800 POWDER MILL RD
ADELPHI MD 20783-1197

1 DIRECTOR
US ARMY RESEARCH LAB
RDRL D
2800 POWDER MILL RD
ADELPHI MD 20783-1197

NO. OF COPIES ORGANIZATION

4 COMMANDER
1 CD US ARMY ARDEC
AMSTA AAR AEM I
G DEROSA
J MIDDLETON
M GONZALEZ
M VOLKMANN
BLDG 65N
PICATINNY ARSENAL NJ 07806-5000

1 US ARMY RDECOM ARDEC
AMSRD AAR AEM L
E LOGSDON
BLD 65
PICATINNY ARSENAL NJ 07806-5000

2 COMMANDER
US ARMY ARDEC
AMSTA AR CCL B
M MINISI
S SPICKERT FULTON
BLDG 65 N
PICATINNY ARSENAL NJ 07806-5000

1 COMMANDER
US ARMY ARDEC
AMSTA AAR AEM I
M NICKOLICH
BLDG 65 N
PICATINNY ARSENAL NJ 07806-5000

1 COMMANDER
US ARMY ARDEC
RDAR QES C
M WESSEL
BLDG 62
PICATINNY ARSENAL NJ 07806-5000

6 PM ARMS
1 CD SFAE AMO MAS SMC
R KOWALSKI
F HANZL
P RIGGS
J LUCID
H KOURLOS
K THOMAS
BLDG 354
PICATINNY ARSENAL NJ 07806-5000

NO. OF COPIES ORGANIZATION

3 CDR USAIC
1 CD SOLDIER REQ DIV
SMALL ARMS BR
LTC HENTHORN
J AMICK
R HARBISON
FORT BENNING GA 31905-5400

1 TRADOC CAPAILITY MANAGER
ATIC TCT
J KORNFELD
BLD 2787, HARRISON LOOP
FORT EUSTIS, VA 23604

1 US ARMY ARDEC
AMSRD AAR AEM L
D VO
BLDG 65 S
PICATINNY ARSENAL NJ
07806-5000

1 US ARMY ARDEC
AMSRD AAR AEM S
S MUSALLI
BLDG 65S
PICATINNY ARSENAL NJ
07806-5000

1 US ARMY ARDEC
AMSRD AAR EMB
R CARR
BLDG 65N
PICATINNY ARSENAL NJ
07806-5000

1 US ARMY ARDEC
AMSRD AAR AEM L
R SAYER
BLDG 65
PICATINNY ARSENAL NJ
07806-5000

2 US ARMY ARDEC
AMSRD AAR AIJ
V SCHISSLER
K SPIEGEL
BLDG 65
PICATINNY ARSENAL NJ
07806-5000

NO. OF
COPIES ORGANIZATION

1 US ARMY ARDEC
AMSTA AR FSP G
D CARLUCCI
BLDG 94
PICATINNY ARSENAL NJ
07806-5000

3 COMMANDER
US ARMY TACOM ARDEC
AMSRD AAR AEM A
C LIVECCHIA
J GRAU
B WONG
BLDG 94
PICATINNY ARSENAL NJ 07806-5000

6 COMMANDER
US ARMY TACOM ARDEC
AMSRD AAR AEM A
G MALEJKO
E VAZQUEZ
W TOLEDO
W KOENIG
S CHUNG
T RECCHIA
BLDG 94S
PICATINNY ARSENAL NJ 07806-5000

5 COMMANDER
US ARMY TACOM ARDEC
AMSRD AAR AEM A
A FARINA
L YEE
R TROHANOWSKY
S HAN
C WILSON
BLDG 95
PICATINNY ARSENAL NJ 07806-5000

ABERDEEN PROVING GROUND

32 DIR USARL
RDRL HRS B
T FRY
RDRL SLB D
R KINSLER
RDRL WM
P PLOSTINS
B FORCH
RDRL WML
J NEWILL
M ZOLTOSKI
RDRL WML A
C MERMAGEN
W OBERLE

NO. OF
COPIES ORGANIZATION

J SOUTH
S WANSACK
D WEBB
RDRL WML E
I CELMINS
G COOPER
J DESPIRITO
F FRESCONI
J GARNER
B GUIDOS
K HEAVEY
J SAHU
S SILTON
P WEINACHT (1 CD, 3 CP)
G OBERLIN
RDRL WML F
D LYON
RDRL WML H
C CANDLAND
T EHLERS
L MAGNESS
RDRL WMM D
R CARTER
RDRL SLB W
P GILLICH
T MEYERS

TOTAL: 80 (4 CDS, 75 HCS, 1 PDF)

INTENTIONALLY LEFT BLANK.